

Efficient Methods for Novel Passive Structures in Waveguide and Shielded Transmission Line Technology

by

Cheng Zhao

Thesis submitted for the degree of

Doctor of Philosophy

in

Electrical and Electronic Engineering,
Faculty of Engineering, Computer and Mathematical Sciences
The University of Adelaide, Australia

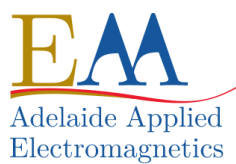
2016

Supervisors:

Assoc Prof Cheng-Chew Lim, School of Electrical & Electronic Engineering

Prof Christophe Fumeaux, School of Electrical & Electronic Engineering

Dr Thomas Kaufmann, School of Electrical & Electronic Engineering



© 2016
Cheng Zhao
All Rights Reserved



*To my dearest father and mother,
with all my love.*

Contents

Contents	v
Abstract	ix
Statement of Originality	xi
Acknowledgments	xiii
Thesis Conventions	xv
Publications	xvii
List of Figures	xix
List of Tables	xxv
Chapter 1. Introduction	1
1.1 Introduction	2
1.2 Objectives of the Thesis	2
1.3 Summary of Original Contributions	4
1.3.1 Band-Pass Filters and Shielded Microstrip Lines	4
1.3.2 New Junctions and Diplexers	7
1.4 Thesis Outline	8
Chapter 2. Literature Review	13
2.1 Introduction	14
2.2 Filters, Transmission Lines and Multiplexers	14
2.2.1 Filters	14
2.2.2 Transmission Lines	18
2.2.3 Multiplexers	20
2.3 Numerical Methods in Electromagnetics	22
2.4 Chapter Summary	25

Chapter 3. Band-Pass Iris Rectangular Waveguide Filters	27
3.1 Introduction	28
3.2 Principle of the Mode-Matching Method for Irises	28
3.2.1 Fields in Rectangular Waveguide	29
3.2.2 Mode-Matching Analysis of Rectangular Waveguide Double-Plane Step Discontinuities	33
3.2.3 Scattering Matrices of Irises Placed in Rectangular Waveguides	39
3.3 Principle of Band-Pass Filter	42
3.3.1 Principle of the Insertion Loss Method	44
3.3.2 Low-Pass Filter Prototype	45
3.3.3 Band-Pass Transformation	48
3.4 Band-Pass Iris Filter	50
3.4.1 Realisation of Band-Pass Iris Filter	50
3.4.2 Influence of Fabrication Inaccuracies	54
3.4.3 Approaches to Remove Undesired Influence	57
3.5 Chapter Summary	63
Chapter 4. Band-Pass Post Rectangular Waveguide Filters	67
4.1 Introduction	68
4.2 Principle of the Mode-Matching Method for Posts	68
4.2.1 Mode-Matching Analysis of Double-Plane Discontinuity with Multiple Apertures	70
4.2.2 Scattering Matrices of N -furlcations Placed in Rectangular Waveguides	72
4.2.3 Mode-Matching Analysis of Posts Placed in a Rectangular Waveguide	77
4.3 General Design for Band-Pass Post Filters in Rectangular Waveguides and Substrate-Integrated Waveguides	86
4.3.1 Structures of Band-Pass Post Filters	86
4.3.2 K Inverter Values Analysis of Posts or Vias	88
4.3.3 Design Examples	89
4.4 Tolerance Analysis	93
4.5 Insertion Losses Analysis	96
4.6 Chapter Summary	104

Chapter 5. Shielded Transmission Lines and Band-Pass Folded Substrate-Integrated Waveguide Filters	107
5.1 Introduction	108
5.2 Mode-Matching Method for Planar and Quasi-Planar Transmission Lines	109
5.3 Mode-Matching Analysis of Dimensions for Single-Mode Operation of Shielded Microstrip Lines	120
5.3.1 Eigenfunction in Shielded Microstrip Lines	121
5.3.2 Analysis of Fundamental Mode in Shielded Microstrip Lines . . .	122
5.3.3 Analysis of the 2 nd -Order Mode in Shielded Microstrip Lines . .	123
5.4 Folded Substrate-Integrated Waveguide and the Application in Band-Pass Post Filter	127
5.4.1 Dispersion Characteristics of Folded Substrate-Integrated Waveguide	128
5.4.2 Posts in Folded and Unfolded Rectangular Waveguide	132
5.4.3 A Novel Band-Pass Post Folded Substrate-Integrated Waveguide Filter	133
5.5 Chapter Summary	137
Chapter 6. Three-Port Junctions and Diplexers	139
6.1 Introduction	140
6.2 Constraints for the Optimum Performance of Diplexers with Symmetric Three-Port Junctions	140
6.3 Novel Three-Port Junctions	145
6.3.1 Optimised Y-Junctions	145
6.3.2 Double-Layer Junction	149
6.3.3 Y-junction in Folded Substrate-Integrated Waveguide Technology	151
6.3.4 Junction with stairs in Folded Substrate-Integrated Waveguide Technology	159
6.4 Novel Diplexers	162
6.4.1 Diplexers with Improved Y-junctions in Substrate-Integrated Waveguide Technology	163
6.4.2 Diplexer with Double-Layer Junctions in Substrate-Integrated Waveguide Technology	168

6.4.3	Diplexer with Junction in T-type and E-type Folded Substrate-Integrated Waveguide Technology	175
6.5	Chapter Summary	181
Chapter 7. Conclusions and Future Work		183
7.1	Introduction	184
7.2	Band-Pass Filters and Shielded Microstrip Lines	184
7.2.1	Original Contributions	184
7.2.2	Future Work	187
7.3	New Junctions and Diplexers	188
7.3.1	Original Contributions	188
7.3.2	Future Work	190
7.4	Closing Comments	190
Bibliography		193
List of Acronyms		205
List of Symbols		207
Biography		213

Abstract

With the rapid development of microwave and millimetre-wave systems, the performance requirements for passive band-pass filters and diplexers, as essential parts in these systems, are steadily increasing. Both rectangular waveguide and substrate-integrated waveguide technologies help to satisfy various high-performance requirements. Rectangular waveguides offer the advantages of low loss and high power handling capabilities, while substrate-integrated waveguides have the advantages of low cost and easy integration into planar circuit technology. Besides, the miniaturisation of electronic devices is of great importance, especially for microwave or millimetre-wave systems whose volume is limited by system considerations. Hence, the two main aims of this thesis are firstly to develop efficient methods which can improve the design reliability and reduce the design cycle of such passive devices, and secondly to present novel structures of band-pass filters and diplexers whose dimensions are reduced.

In the first part of the thesis, a method based on the mode-matching technique is developed to rigorously and efficiently analyse the negative influence introduced by micro-machining errors on the performance of band-pass H-plane iris filter. This analysis includes the effect on the centre frequency and 3 dB bandwidth caused by the round angles between waveguide walls and H-plane irises, or by the bevel angles on the H-plane irises. To remove these undesired influences, three approaches are proposed and verified with simulations performed with the finite-element method.

In the next part, efficient approximation approaches are investigated in the framework of the mode-matching method to analyse the characteristics of cylindrical posts placed in the cross-section of a rectangular waveguide or substrate-integrated waveguide. Compared with the H-plane irises in rectangular waveguides, cylindrical posts are more promising for realising band-pass rectangular waveguide filters, because the geometries are easier to manufacture and less prone to machining errors. Thus, a general design procedure for band-pass post filters in rectangular waveguides and substrate-integrated waveguides is developed and verified with finite-element simulations and measurements on prototypes. The tolerance analysis for the band-pass filters is also explored quickly and accurately with the developed method, while the influence of realistic material losses on the insertion loss of various structures, is also quantitatively

analysed with a full-wave simulation solver.

Next, the characteristics of a shielded microstrip line for single-mode operation is investigated rigorously based on the mode-matching method. The research focuses on the influence of the metal enclosure dimensions on the fundamental mode, and the relationships between the cutoff frequency of the 2^{nd} -order mode and the geometrical variables of the cross-section of the shielded transmission line. A similar method is then applied to an E-type folded substrate-integrated waveguide. The analysis demonstrates that the propagation characteristics for the first twenty modes in the E-type folded substrate-integrated waveguide and its corresponding equivalent rectangular waveguide are almost identical if the width of the middle metal vane in the E-type folded substrate-integrated waveguide is chosen reasonably. Exploiting this similarity property, a novel concept of band-pass post filter in E-type folded substrate-integrated waveguide technology is developed to reduce the band-pass filter dimension further, together with an efficient specific design procedure. The validity of the approach is verified via finite-element simulations and measurements on a fabricated prototype.

Finally, to reduce the sizes of common diplexers, four types of novel three-port junctions are proposed, including two improved Y-junctions in substrate-integrated waveguide technology, a double-layer junction in substrate-integrated waveguide technology, a Y-junction in T-type folded substrate-integrated waveguide technology, and a junction with stairs in T-type and E-type folded substrate-integrated waveguide technology. Exploiting the flexibility of the in-house developed mode-matching code or a commercial finite-element simulation solver, the characteristics for all presented junctions are shown to satisfy the constraints for optimum performance of diplexers when adjusting the relevant variables in the corresponding structures. Three types of these junctions are then utilised in realising diplexers whose performance is verified over the required operation bands with either numerical simulations or measurements on fabricated prototypes.

In summary, this thesis has introduced novel concepts and realisations of compact band-pass filters and diplexers in unfolded or folded substrate-integrated waveguide technology, as well as related structures. One of the crucial aspects emphasised throughout the research is the need for efficient and accurate modelling methods specifically tailored to support such developments. This has been demonstrated throughout the thesis with the combined use of powerful numerical methods and equivalent models based on symmetries or unfolded geometries.

Statement of Originality

I certify that this work contains no material, which has been accepted for the award of any other degree or diploma in my name, in any university or other tertiary institution and, to the best of my knowledge and belief, contains no material previously published or written by another person, except where due reference has been made in the text. In addition, I certify that no part of this work will, in the future, be used in a submission in my name, for any other degree or diploma in any university or other tertiary institution without the prior approval of the University of Adelaide and where applicable, any partner institution responsible for the joint-award of this degree.

I give consent to this copy of my thesis when deposited in the University Library, being made available for loan and photocopying, subject to the provisions of the Copyright Act 1968.

The author acknowledges that copyright of published works contained within this thesis resides with the copyright holder(s) of those works.

I also give permission for the digital version of my thesis to be made available on the web, via the University's digital research repository, the Library Search and also through web search engines, unless permission has been granted by the University to restrict access for a period of time.

Signed

23/03/2016

Date

Acknowledgments

First and foremost, I would like to express my sincere gratitude to my supervisors Assoc Prof Cheng-Chew Lim, Prof Christophe Fumeaux and Dr Thomas Kaufmann for their continuous guidance and support during my candidature. My principal supervisor, Assoc Prof Cheng-Chew Lim accepted me as a PhD candidate in 2012. His immense and professional knowledge, serious and responsible attitude, patient and enthusiastic supervision, and constructive suggestions provided significant help in advancing my research. From the third year of my candidature, I was honoured to be one of Prof Christophe Fumeaux's students, who is an expert in microwave and millimetre-wave engineering and computational electromagnetics. He was always glad to share his extensive knowledge and abundant experimental experience, and welcomed scientific enquiries and discussions. My research work benefited a lot from his technical support, insightful advices, and meticulous feedback. Another co-supervisor whom I am genuinely indebted to is Dr Thomas Kaufmann. His deep theoretical knowledge, insightful comments, and encouragement were of great importance towards my research.

In addition to my supervisors, I would like to convey my gratitude to my friends and colleagues in the Adelaide Applied Electromagnetics Group in School of Electrical & Electronic Engineering at the University of Adelaide, Dr Ali Karami Horestani, Dr Zahra Shaterian, Dr Amir Ebrahimi, Mr Shengjian (Jammy) Chen, Dr Tiaoming (Echo) Niu, Mr Nghia Nguyen-Trong, Dr Withawat Withayachumnankul, Mr Chengjun Zou, Ms Wendy Suk Ling Lee, and Mr Sree Pinapati, to my advisor, Dr Yingbo Zhu, and to the professional staff, Mr Brandon F. Pullen, Mr Pavel Simcik, Mrs Rose-Marie Descalzi, and Mr David Bowler.

I would also like to express my heartfelt thanks to my best friends, Mr Ming Chen and Mr Qianwen Xia, for your warmest wishes, and your appearing in my life and keeping me company.

This thesis was made possible by an Australian Postgraduate Award Scholarship. I am sincerely indebted to the Department of Education and Training of Australian Government, which gave me the opportunity to undertake a PhD program at the University of Adelaide.

Acknowledgments

Last but not least, my endless love and appreciation goes to my parents who gave birth to me, raised and educated me with continuous love and patience, and were supporting and encouraging me infinitely.

Cheng Zhao,
March 2016,
Adelaide

Thesis Conventions

The following conventions have been adopted in this Thesis:

Typesetting

This document was compiled using $\text{\LaTeX}2\text{e}$. Texmaker and TeXstudio were used as text editor interfaced to $\text{\LaTeX}2\text{e}$. Inkscape and Xcircuit were used to produce schematic diagrams and other drawings.

Referencing

The Harvard style has been adopted for referencing.

System of units

The units comply with the international system of units recommended in an Australian Standard: AS ISO 1000–1998 (Standards Australia Committee ME/71, Quantities, Units and Conversions 1998).

Spelling

Australian English spelling conventions have been used, as defined in the Macquarie English Dictionary (A. Delbridge (Ed.), Macquarie Library, North Ryde, NSW, Australia, 2001).

Publications

Journal Articles

ZHAO-C., FUMEAUX-C., AND LIM-C. C. (2016b). Substrate-Integrated Waveguide (SIW) Diplexers with Improved Y-junctions, *Microwave and Optical Technology Letters*, 58(6), pp. 1384–1388.

Conference Articles

ZHAO-C., FUMEAUX-C., AND LIM-C. C. (2016a). Folded Y-junction in Substrate-Integrated Waveguide Technology, *The 2nd Australian Microwave Symposium*.

ZHAO-C., FUMEAUX-C., KAUFMANN-T., ZHU-Y., AND LIM-C. C. (2015b). Mode Matching Analysis of Dimension for Single-Mode Operation of Shielded Microstrip Lines, *2015 Asia-Pacific Microwave Conference (APMC)*, Vol. 2, pp. 1–3.

ZHAO-C., FUMEAUX-C., AND LIM-C. C. (2015a). Losses in Substrate Integrated Waveguide Band-Pass Post Filters, *2015 Asia-Pacific Microwave Conference (APMC)*, Vol. 2, pp. 1–3.

ZHAO-C., FUMEAUX-C., KAUFMANN-T., ZHU-Y., HORESTANI-A. K., AND LIM-C. C. (2015c). General Design Method for Band-pass Post Filters in Rectangular Waveguide and Substrate Integrated Waveguide, *International Symposium on Antennas and Propagation (ISAP2015)*, pp. 946–949.

ZHAO-C., KAUFMANN-T., ZHU-Y., AND LIM-C. C. (2014a). Approximation Methods for Cylindrical Posts in Rectangular Waveguides with Mode Matching Technique, *2014 IEEE Asia-Pacific Conference on Applied Electromagnetics (APACE)*, pp. 179–182.

ZHAO-C., KAUFMANN-T., ZHU-Y., AND LIM-C. C. (2014b). Efficient Approaches to Eliminate Influence Caused by Micro-Machining in Fabricating H-Plane Iris Band-Pass Filters, *2014 Asia-Pacific Microwave Conference (APMC)*, pp. 1306–1308.

Article in Review

ZHAO-C., FUMEAUX-C., AND LIM-C. C. (n.d.). Folded Substrate-Integrated Waveguide Band-pass Post Filter, *IEEE Microwave and Wireless Components Letters*. Accepted on 1 July 2016, Subject to revision.

List of Figures

1.1	Thesis outline	9
<hr/>		
2.1	Network of Campbell's low-pass filter	15
2.2	Structure of the first cross-coupled filter	17
2.3	Three types of transmission line models	19
2.4	Commonly used types of printed transmission lines	20
2.5	Schematic structure of a multiplexer	21
<hr/>		
3.1	Structure of a W-band 5-cavity band-pass H-plane iris rectangular waveguide filter	29
3.2	Common iris discontinuities in rectangular waveguide and their equivalent circuits	30
3.3	Electric and magnetic fields for the TE ₁₀ mode in a rectangular waveguide	31
3.4	A double-plane step discontinuity in rectangular waveguide	33
3.5	Wave amplitude coefficients at the junction between waveguide I and II	34
3.6	A resonant iris placed in the cross-section of a rectangular waveguide . .	40
3.7	Symmetric H-plane iris placed in the cross-section of a rectangular waveguide	42
3.8	Relationship between the convergence and the number of adopted modes at 94 GHz	43
3.9	Comparison for the amplitude and phase of scattering parameters obtained through the MMM with 15 modes and the FEM using Ansys HFSS in W-Band	44
3.10	Chebyshev (equal ripple) low-pass response for filters with $N = 3$, $N = 5$, and $N = 7$ orders	46
3.11	Two types of ladder networks for all-pole low-pass filters	47
3.12	Two types of networks for band-pass filters transformed from ladder networks for low-pass filters	49

List of Figures

3.13	Network for generalised band-pass filter using impedance inverters . . .	51
3.14	Structure of a 5 th -order Chebyshev band-pass iris filter	52
3.15	An iris placed in the cross-section of a rectangular waveguide and the equivalent circuit for the impedance inverter	53
3.16	Comparison of scattering parameters obtained using MMM and the FEM using Ansys HFSS	55
3.17	Structure of a 5 th -order Chebyshev band-pass iris filter with round angles	56
3.18	Irises with different types of fabrication effects taken into account: (a) round angles, (b) bevel angles	57
3.19	Relationship between the convergence and the number of steps for an iris with (a) round angles and (b) bevel angles at 94 GHz	58
3.20	Relationship between the radius or side length, the offset of the centre frequency, and the variation of bandwidth	59
3.21	Comparison of scattering parameters obtained using the MMM and the FEM using Ansys HFSS	61
3.22	An iris with both rounded angles and bevel angles and its equivalent circuit for the impedance inverter	62
3.23	Comparison of scattering parameters obtained using the MMM and the FEM using Ansys HFSS	63
3.24	Comparison of scattering parameters obtained using the MMM and the FEM using Ansys HFSS	64
<hr/>		
4.1	Structures of X-band 5-cavity band-pass (a) post rectangular waveguide filter, and (b) via SIW filter	69
4.2	A double-plane step discontinuity with two apertures	72
4.3	Two H-plane inserts placed in the cross-section of a rectangular waveguide	73
4.4	Schematic diagrams of an <i>N</i> -furcation rectangular waveguide structure	74
4.5	Relationship between the convergence and the number of adopted modes at 94 GHz	75
4.6	Comparison for the amplitude and phase of scattering parameters obtained through the MMM with 25 modes and the FEM using Ansys HFSS in W-Band	76

4.7	Half part of a symmetric 3-furcation structure shown in Fig. 4.3	77
4.8	Method A (equal width method): approximation of cross-section by (a) over-estimating, (b) under-estimating the circle and (c) averaging the previous two approaches	78
4.9	Method B (arithmetic sequence thickness method): approximation of cross-section by (a) over-estimating, (b) under-estimating the circle and (c) averaging the previous two approaches	79
4.10	Method C (equal sector method): approximation of cross-section by (a) over-estimating, (b) under-estimating the circle and (c) averaging the previous two approaches	80
4.11	Scattering parameter convergences: (a) equal width method, (b) arithmetic sequence thickness method and (c) equal sector method	82
4.12	Difference between scattering parameters and accurate reference values: (a) equal width method (over), (b) equal width method (under), (c) equal width method (average), (d) arithmetic sequence thickness method (over), (e) arithmetic sequence thickness method (under), (f) arithmetic sequence thickness method (average), (g) equal sector method (over), (h) equal sector method (under), and (i) equal sector method (average)	83
4.13	Comparison between the MMM and the FEM using Ansys HFSS	84
4.14	Realisations of 5-cavity band-pass filters: (a) post rectangular waveguide filter, (b) via SIW filter	87
4.15	Posts placed in the cross-section of a rectangular waveguide and the equivalent circuit for the impedance inverter	88
4.16	Relationships of K factors, radii r and distances $G/2$ to the magnetic wall	90
4.17	Fabricated 5-cavity Chebyshev band-pass post filters	91
4.18	Comparison of scattering parameters obtained using the MMM, the FEM (Ansys HFSS), and measurements	94
4.19	Offset Δf_c of centre frequency and variation $\Delta f_{3\text{dB}}$ of 3 dB bandwidth caused by machining errors	95
4.20	Comparison of scattering parameters between the simulation results for two sets of band-pass SIW filters	99
4.21	Comparison of scattering parameters obtained using the FEM (Ansys HFSS) and measurements	100

List of Figures

4.22	Generic structure of an N^{th} -order Chebyshev band-pass post SIW filter .	100
4.23	Influence caused by the metal conductivity, the dielectric loss tangent, and the thickness of the substrate on the insertion losses of band-pass SIW filters realised in RT/duroid 6002 (dashed lines) and RT/duroid 6006 (solid lines) at 10.5 GHz	103
<hr/>		
5.1	Structure of a planar or quasi-planar transmission line for microwave, millimetre-wave and optoelectronic applications	108
5.2	Cross-section of the shielded microstrip transmission line	121
5.3	Influence on the fundamental mode of varying (a) the width a and (b) the height b of the shielding housing	124
5.4	Comparison of the fundamental mode's phase constant at 94 GHz between a microstrip line without housing and a shielded microstrip line .	125
5.5	Influence on the cutoff frequency of the 2^{nd} -order mode caused by the geometry and the relative permittivity of the substrate	126
5.6	Structure of an E-type FSIW and its equivalent folded dielectric-loaded rectangular waveguide	128
5.7	Relationship between the cutoff frequency of the first even mode in FSIW and the length of the middle vane	130
5.8	Electric fields of the first even mode at 10 GHz when the length c of the middle vane is 4.74 mm, 9.68 mm, and 10.05 mm	130
5.9	Comparison of the even modes' phase constants of the folded rectangular waveguide with corresponding modes of the unfolded rectangular waveguide when the length c of the middle vane is 9.68 mm	131
5.10	Structures for posts placed in the cross-section of a folded and an unfolded rectangular waveguide	132
5.11	Comparison of (a) $ S_{11} $ and (b) $ S_{21} $ between posts with different radii r placed in the cross-section of a folded rectangular waveguide and the equivalent unfolded rectangular waveguide	133
5.12	Structure of a 5-cavity Chebyshev band-pass post filter realised in: (a) FSIW technology, (b) and its equivalent structure in SIW technology . .	135
5.13	Comparison of scattering parameters between the band-pass post FSIW filter and its equivalent unfolded rectangular waveguide band-pass filter	136

5.14	Fabricated FSIW band-pass post filter (bottom and top substrates)	137
<hr/>		
6.1	Structure of a common T-junction rectangular waveguide diplexer	141
6.2	Configuration of a diplexer modelled as a lossless three-port junction and two band-pass filters	142
6.3	Structures of (a) a Y-junction with two bends, and (b) its approximation steps including an H-plane step and a bifurcation step in a dielectric-loaded rectangular waveguide	147
6.4	Comparison between scattering parameters ($ S_{11} $, $ S_{22} $, and $ S_{33} $) of Y-junction with bends calculated using the MMM and those of Y-junction without bends obtained using Ansys HFSS when (a) $L_b = 3$ mm, and (b) $L_b = 8$ mm	148
6.5	Structures of Y-junctions improved by (a) tuning the output branch angle φ_1 and (b) inserting vias into the junction	149
6.6	Scattering parameters obtained using the MMM for (a) improved Y-junction 1 and (b) improved Y-junction 2	150
6.7	Structures of (a) a double-layer three-port SIW junction and (b) its equivalent model	152
6.8	Elements used to form a double-layer three-port junction	153
6.9	Characteristics of the double-layer three-port junction when the width g_s of the coupling slot is 0.1 mm, 0.45 mm, and 2.0 mm	154
6.10	Structure of Y-junction realised in: (a) FSIW technology, and (b) SIW technology	155
6.11	Cross-sections of equivalent solid-wall (a) folded waveguide and (b) unfolded waveguide	156
6.12	Comparison between the first twenty modes' phase constants of the folded rectangular waveguide and the corresponding modes of the unfolded rectangular waveguide	156
6.13	Scattering parameters of the folded and unfolded rectangular waveguide Y-junction with 120° angles	157
6.14	Influence on reflection coefficients caused by variations of (a) the width and (b) the thickness of the middle vane	158

List of Figures

6.15	Structures of a symmetric three-port junction formed with T-type and E-type FSIWs and its equivalent model	159
6.16	Scattering parameters of the three-port junction formed with T-type and E-type FSIWs	162
6.17	Structures of two diplexers with improved bent Y-junctions	164
6.18	Scattering parameters calculated using the MMM for (a) Filter 1 and (b) Filter 2	166
6.19	Comparison of scattering parameters obtained using the MMM (without considering losses and effect of transitions), the finite-element method Ansys HFSS and measurements for (a) Diplexer 1 and (b) Diplexer 2	168
6.20	Fabricated diplexers with improved Y-junctions	169
6.21	Structure of a diplexer realised in double-layer three-port junction	171
6.22	Scattering parameters calculated using the MMM for (a) Filter 1 and (b) Filter 2	173
6.23	Two common approaches to eliminate the unwanted bend discontinuity effect for transmission lines with (a) rounded corner (b) chamfered corner	174
6.24	Comparison of scattering parameters obtained using the MMM (without considering losses, effect of transitions, and SMA connectors), and Ansys HFSS (considering losses, effect of transitions, and SMA connectors)	175
6.25	Structures of (a) the diplexer in FSIW technology and (b) the T-type FSIW-to-microstrip transmission	177
6.26	Comparison between scattering parameters simulated using Ansys HFSS for FSIW filters and that calculated using the MMM for the corresponding unfolded filters	179
6.27	Scattering parameters for the diplexer in T-type and E-type FSIW technology obtained using Ansys HFSS	180

List of Tables

2.1	Comparison of Numerical Methods	25
3.1	Dimensions of a 5 th -order Chebyshev band-pass iris filter (Units: mm) .	54
3.2	Dimensions of a 5 th -order Chebyshev band-pass iris filter with round angles (Units: mm)	60
3.3	Dimensions of a 5 th -order Chebyshev band-pass iris filter with both round angles and bevel angles (Units: mm)	64
4.1	Scattering parameters at 94 GHz (Units: dB)	81
4.2	Minimum number of steps M to limit the errors of $ S_{21} $ in ± 0.1 dB or ± 0.05 dB (Units: dB)	85
4.3	Computation time and scattering parameters comparisons	85
4.4	Dimensions of a 5 th -order Chebyshev band-pass post filter in rectangular waveguide technology (Units: mm)	92
4.5	Dimensions of a 5 th -order Chebyshev band-pass via filter in SIW technology (Units: mm)	93
4.6	Filters designed with RT/duroid 6002 (Units: mm)	97
4.7	Filters designed with RT/duroid 6006 (Units: mm)	98
4.8	Insertion losses at 10.5 GHz introduced by different components of the N^{th} -order filters realised in RT/duroid 6002	101
4.9	Insertion losses at 10.5 GHz introduced by different components of the N^{th} -order filters realised in RT/duroid 6006	102
5.1	Parameters of a shielded microstrip transmission line	123
5.2	Sizes of an FSIW band-pass post filter (Units: mm)	134
6.1	Sizes of improved Y-junctions (Units: mm or degree)	151
6.2	Dimensions of the junction with stairs in T-type and E-type FSIW technology (Units: mm)	163
6.3	Synthesized parameters of the designed Chebyshev 3 rd -order band-pass SIW via filters (Units: mm)	165

List of Tables

6.4	Dimensions of an SIW-to-microstrip transition and the distances between filters and junction ports (Units: mm)	167
6.5	Synthesized parameters of the designed Chebyshev 3 rd -order band-pass SIW via filters (Units: mm)	172
6.6	Dimensions of an SIW-to-microstrip transition, the side of the chamfered corner, and the distances between filters and junction ports (Units: mm)	172
6.7	Synthesized parameters of the designed Chebyshev 5 th -order band-pass via FSIW filters (Units: mm)	178
6.8	Dimensions of a T-type FSIW-to-microstrip transition, and the distances between filters and the junction ports (Units: mm)	180